Journal of Multidisciplinary Sciences
www.multidisciplines.com

Delineation of subsurface structural trends and depth of basement of Kattaniya inversion north western desert, Egypt: aeromagnetic data

Abdel Nasser R. Abuzied[1*], Abdelhay A. Farrag[2], Ali M. Abd-Allah[3] and Mohamed H. Abd El-Aal[4]

[1]Geology Department, Faculty of Science, New Valley University, Kharga, 72511, Egypt.
[2]Geology Department, Faculty of Science, Assuit University, Assuit, 71516, Egypt.
[3]Geology Department, Faculty of Science, Ain Shams University, Cairo, 11517, Egypt.
[4]Biology and Geology Department, Faculty of Education/ Ain Shams University, Cairo, 11517, Egypt.
**Corresponding author email address: nasserabuzied@yahoo.com*

Received: 02 December 2021; Accepted: 18 February 2022; Published online: 26 February 2022

Abstract. The area under investigation is located in the northeastern Western Desert and northwest Beni-Suef, covering Kattaniya inversion, Gindi basin, El-Fayum depression, and Wadi Al – Rayan area. It is extended to the east of the River Nile and bounded by Latitudes 29° N and 30° 30` N and Longitudes 29° 15` E and 31° 30` E. This study aims to delineate the subsurface structures and determine the depth of the basement complex in the area under investigation. The conversion of total intensity aeromagnetic data reduced to pole (RTP) magnetic intensity is the first step in achieving these objectives. Subsequently, multiple transformation methods and various filtering operations are applied to magnetic data through descriptive and analytical evaluations. Two methods have been applied on RTP aeromagnetic data to estimate the depth of basement and subsurface structure elements, the first method is power spectrum analysis, and the second method is 2D modeling. The (RTP) magnetic data have been spectrally split into regional and residual magnetic components by applying the estimated power spectrum technique. The average depths of both shallow and deep sources derived from the power spectrum are 3.5 km and 1.17 km. The study area's trends and structural styles are NE-SW, E-W, N-S, NW-SE, and ENE trends.

Keywords: *Kattaniya, aeromagnetic, 2D modeling, and radial power spectrum.*

Cite this as: Abuzied, A.N.R., Farrag, A.A., Abd-Allah, A.M. & Abd El-Aal, M.H. (2022). Delineation of subsurface structural trends and depth of basement of Kattaniya inversion north western desert, Egypt: aeromagnetic data. J. Multidiscip. Sci. 4(1), 25-32.

1. Introduction

The study area under investigation is located in the northern part of the western desert (Figure 1). The main objectives of this study are to delineate the trends and style of the subsurface structures and determine the depth to the basement surface from the airborne magnetic data.

A magnetic investigation is a valuable tool for identifying the geological features of the subsurface basement (relief and subsurface structure). The variation in the geomagnetic field affected by changes in the proportion of magnetite in the rock is mapped using this method. Sedimentary rocks are usually nonmagnetic and have minimal influence, whereas basic and ultrabasic igneous rocks have more variety and can be used to investigate the bedrock geology hidden beneath cover strata. (Mekonnen, 2004).

Several techniques and methods have been applied to the magnetic data used in the present study: (1) reducing the total intensity magnetic data to the north magnetic pole; (2) isolating the magnetic data into residual and regional components using Fast Fourier Transformation (FFT) techniques; (3) redialing, and (4) two-dimensional magnetic forward modeling along six selected RTP magnetic profiles.

The depth to the basement surface and the underlying structures that may potentially align the overlying sediments are all factors in basement configuration. The Geosoft Oasis Montaj (2008) package applies these methods in the wave vector domain.

Basement depth in the area under investigation of available four boreholes was employed as a critical limitation for the modeling operations. The GM-SYS modeling tool used forward and inverse modeling to update and refine the 2-D starting models (Geosoft Oasis Montaj, 2008; GM-SYS, 2013).

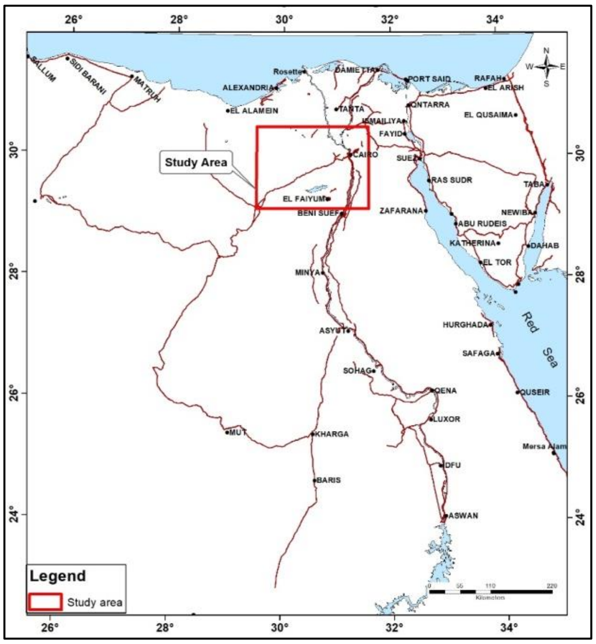

Figure 1. Location map of the investigated area

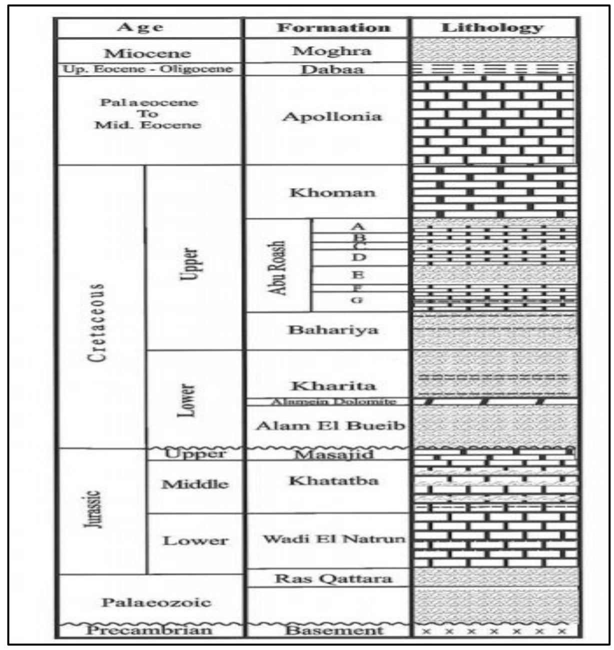

Figure 2. Simplified stratigraphic section of area under investigation modified after Shlumberger (1984) and EGPC (1992).

2. Geological and Structural Setting

The thickness of individual rock units changes in various parts of the area, under investigation in response to the prevailing tectonics at the time of deposition. The stratigraphic section penetrated the area includes a Paleozoic to Recent sedimentary section overlying the Precambrian crystalline basement rocks (Figure 2). This sedimentary section also includes some volcanic at different intervals.

Tectonically, the area described by Mostafa et al. (2008): from detailed structural mapping using borehole and seismic data and isopach of the different rock units in the study area indicates the existence of different tectonic elements in the area. These are, from south to north as the following:

a) WadiEl Rayan platform ENE-WSW oriented belt of normal faults. Faults separate the platform from the Beni Sueif Basin. These down-to-the-souths.
b) Gindi Basin represents a deep fore area lying to the south in the basin is dissected by NW-SE oriented normal faults of post-Eoceneageof the Kattaniya inverted basin. The Apollonia Formation.
c) Kattaniya inverted basin is a major tectonic element in the study area and has a NE-SW orientation. Structurally, it is the highest part of the studied region. During basin subsidence, the Jurassic and Cretaceous rift basin site received a sizeable sedimentary section.

d) Tiba-Natrun basin has a WNW-ESE orientation and lies to the NW of the Kattaniya Basin.

3. Data processing and Interpretation

The total magnetic intensity data (TMI) of the area under investigation were generated from a 2.9 km × 2.9 km grid (Figure 3). The magnetic data was constrained to the magnetic pole to avoid the unwanted deformation of magnetic anomaly shapes, sizes, and locations caused by the inclination of Earth's magnetic field. A reduction to pole (RTP) magnetic map was created using the magnetic field characteristics at this site (I = 45.5, D = 2) (Figure 4). Using Geosoft Oasis Monta's (2008) Package's Fast Fourier Transform (FFT), frequency analysis and analyzers were performed on magnetic data in the spectral domain. The regional and residual elements of the magnetic anomaly were determined using a power spectral technique. The GM-SYS modeling tool was then used to perform two-dimensional forward modeling on 6 selected profiles. The original model was built using all deduced and accessible well data. A significant positive magnetic anomaly going N-S with a peak value of roughly 120 nT distinguishes the west side. A continuation of this positive anomaly may be seen in the map's middle and southern, eastern regions. A magnetic belt formed of negative anomalies and aligned nearly N-S and NE with a minimal magnetic value of -100 nT runs through the area's middle to north, south, northeastern, and eastern regions.

4. Regional-residual Separation

Local anomalies are usually of primary importance in the magnetic survey, and the first step in interpreting is to remove the general field to identify the remaining anomalies. Griffin (1949) first defined the methodology, which estimates the regional field that produces adequate results.

Using the frequency bands defined by the spectrum analysis, low-pass and bandpass filter processes were used to the RTP magnetic data of the area of study to obtain regional (Figure 5) and residual (Figure 6) magnetic element maps. The regional map (Figure 5) matches the RTP magnetic anomaly map regarding the anomaly trend. This correlation shows that most of the relevant magnetic sources in the survey area are of deep-seated origin, i.e., supra-basement structures. Various high-frequency, low-amplitude positively and negatively anomalies moving in N-S and NW-SE directions can be seen on the residual magnetic map (Figure 6).

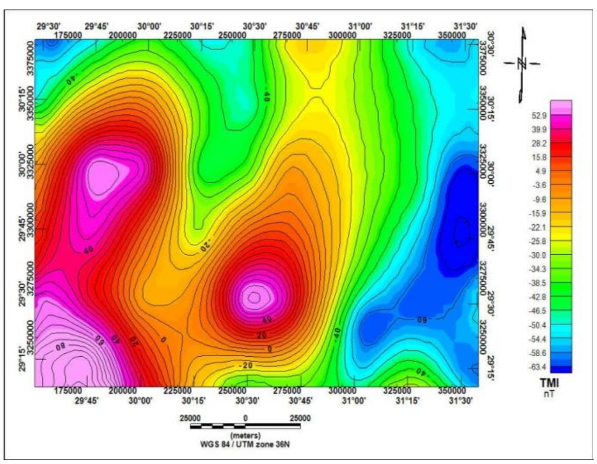

Figure 3. Total Intensity magnetic map of the study area, Northern Western Desert, Egypt.

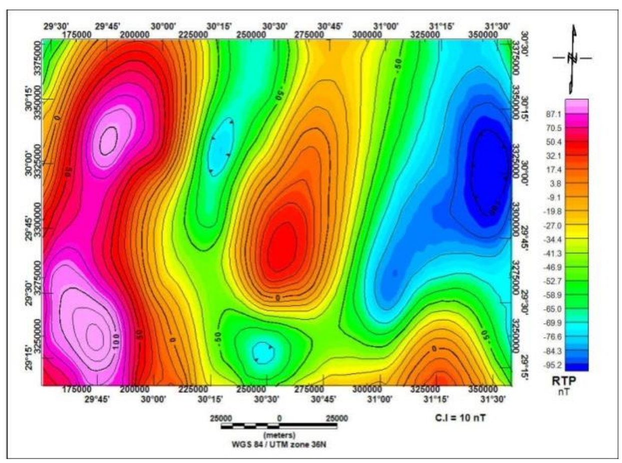

Figure 4. RTP magnetic map of the investigated area.

These anomalies could be due to minor differences in basement rock morphology or the action of basaltic flows entities with varying depths, which are found in the investigated area.

The generation of residual maps is one of the most well-known methods for quantitatively exploring a potential map, in which the measured field includes influences from all nearby bodies. Geophysicists have utilized residual maps to bring small characteristics into emphasis that are often overshadowed by the field's more prominent features (Ammar et al., 1988). Various adverse (green and blue colored) and cheerful (red-colored) magnetic anomalies are visible on the High-pass (residual) filtered map (Figure 5). A few anomalies are elongated, while some are semicircular, and both have a generalized N-S and NW-SE direction. Some faults cut through these zones in various directions. Tectonic subsidence could reflect various basement rocks at the subsurface or in shallow basins.

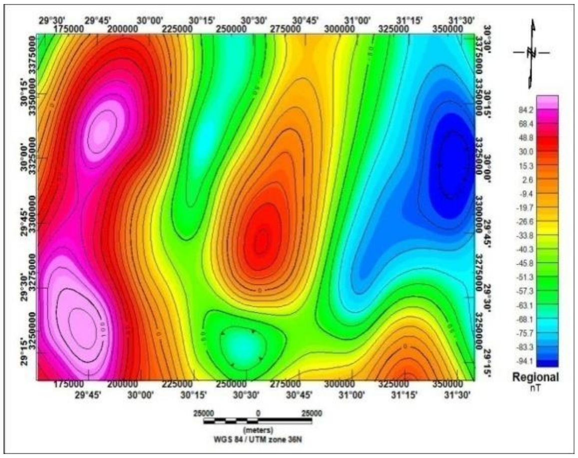

Figure 5. Regional magnetic component of RTP of the investigated area.

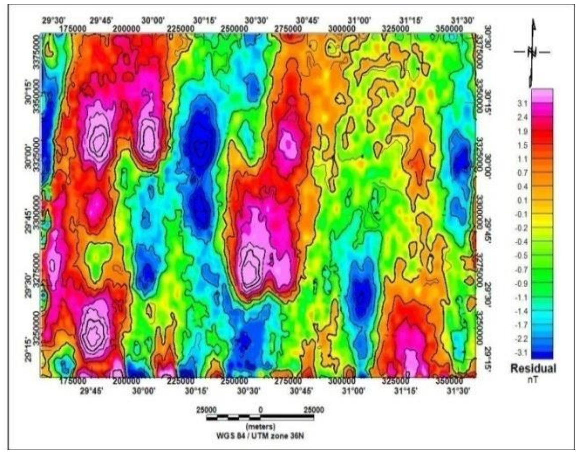

Figure 6. Residual magnetic component of RTP of the investigated area.

5. Analysis of Power Spectrum Transformation

The radial average power spectrum technique is applied to estimate the depths of basement rocks and underlying geological structures. The Fast Fourier Transform (FFT) is used to determine the energy spectrum of the RTP magnetic data in the present study. Numerous publications demonstrate that the spectral analysis method focuses on the findings of magnetic data using the Fourier Transform, including Bhattacharyya (1965), Spector and Grant (1970), Garcia and Ness (1994), and Maurizio et al. (1998).

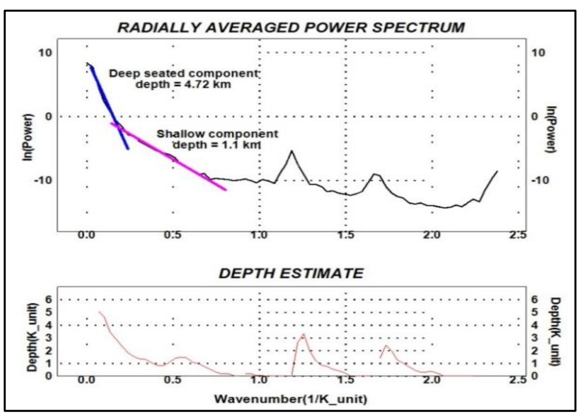

Figure 7. Radially averaged power spectrum of one cell and depth estimate of the RTP magnetic map of the investigated area.

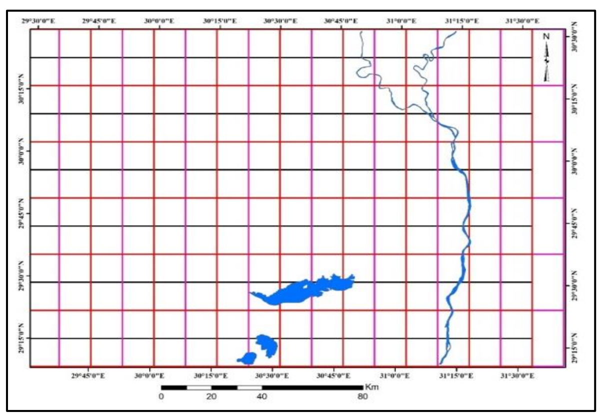

Figure 8. Layout of divided cells with dimensions 25 × 25 km

Graph, the energy spectrum versus frequency on a logarithmic scale, is used to show the result of this process. Figure 7 displays two main components as straight-line segments with decreasing slopes as frequency increases. The depth of each source group responsible for each sector was determined by plugging the segment's slope into the formula:

H (depth) = slope/4π

Applying this technique to the entire area gives a rough general or average depth estimation of shallow and deep sources of basements; therefore, the total area has been divided into smaller cells with dimensions 25 × 25 km (Figure 8). Then applying this method to each cell and put result values in the center of each cell. Both regional deep and residual shallow sources have average depths of 3.5 and 1.17 kilometers, respectively.

6. Structural Style and Interpretation

Mapping of structural trends of a basement depends on a proper depth map to the basement, which was derived from RTP data using the power spectrum analysis of each cell in (Figure 8), where each cell has its specific value representing the depth to the basement. The depth map of the basement has been constructed by contouring these values of power spectrum from each cell and using depth values to the basement from wells that are to constrain the results. Depth map of the basement (Figure 9) illustrates different styles of structural trends. The NE-SW trend refers to Kattaniya high as a regional trend of faults separating the Wadi Natrun basin to the north and the Gindi basin to the south of Kattaniya high. Also the NE trend is correlated on the surface as NE elongated basaltic extrusive. The E-W trend is supported on the surface with the north Galala trend. This trend separates the Gindi basin and Wadi Al-Rayan platform. The ENE trend is shown on the basement's depth map that separates the Wadi Al-Rayan platform and the Benisueif basin south of the area. Also N-S and NW-SE are illustrated on the map. All these regional trends of the structural style of the area are illustrated by a rose diagram (Figure 10).

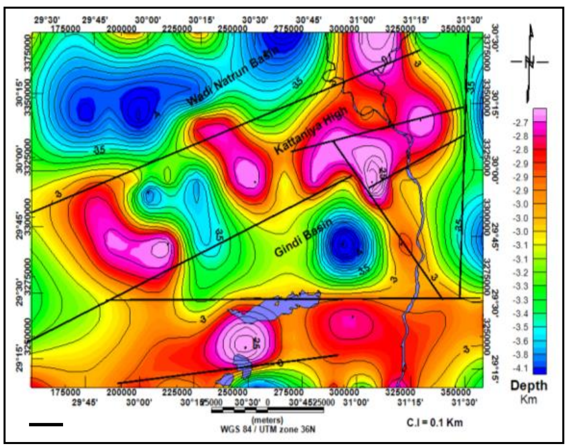

Figure 9. Depth map of basement and subsurface structural style of the investigated area.

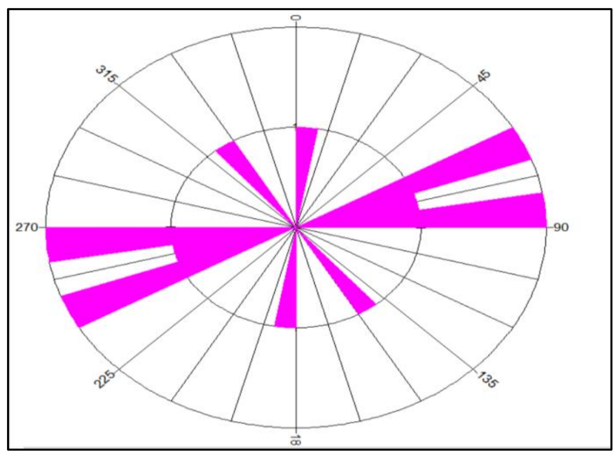

Figure 10. Rose diagram showing main subsurface structural trends of the investigated area.

7. 2D Forward Modeling of Aeromagnetic Data

The GM-SYS modeling tool was used to undertake two-dimensional forward modeling along the examined profiles (Figure 11) to evaluate and enhance magnetic interpretation. These profiles cross at the Wadi El Natrun-1, Alzharaa-1, and Q2-1. The magnetic model response was calculated using the techniques of Talwani et al. (1959) and Talwani and Heirtzler (1964). The sedimentary overlay is given a susceptibility value of zero (cgs units) in all profiles, while the basement rocks are given a value ranging from 0.006 to 0.009 (cgs units).

Figures 12-17 illustrate the 2D modeled profiles. The observed RTP magnetic profile is depicted as a black circle on the upper half of the picture, while the computed magnetic data are drawn as solid black dots superimposed on the observed RTP data. The degree of error is also represented as a red line in the upper part of the model. The computed cross-section is shown in the lower part of the model, and the horizontal X-axis reflects the profile's horizontal distance in kilometers. Two distinct portions are shown on the vertical Y-axis. The upper part is the magnetic anomaly scale in nanoteslas (nT), and the lower part is the depth scale in meters.

The results were obtained from 2D profiles (P1, P2, P3, P4, P5 and P6) are listed in Table 1.

Table 1. Summarized results of 2D Magnetic Modeling				
Profile No.	**Profile direction**	**Profile length (km)**	**Basement depth (m)**	**Errors %**
P1	S - N	150	1500-2750	1.434
P2	S - N	150	3500-4250	1.332
P3	S - N	150	2500-4000	1.5
P4	W - E	200	1900-4400	1.862
P5	W - E	200	200-6250	1.874
P6	W - E	200	750-3500	1.911

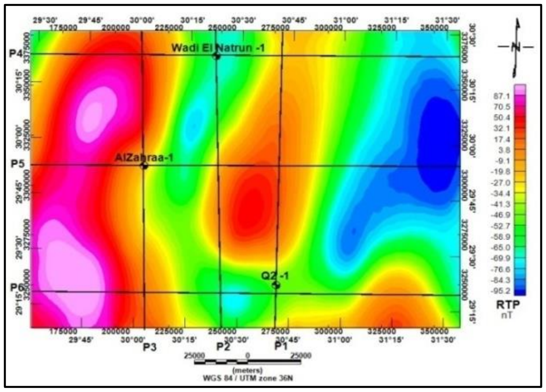

Figure 11. Location map of 2D magnetic profiles of the investigated area.

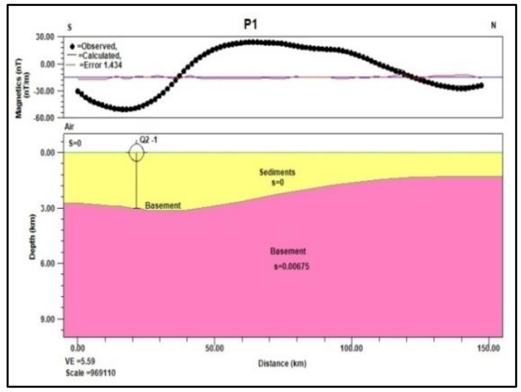

Figure 12. 2D modeled magnetic profile 1of the investigated area.

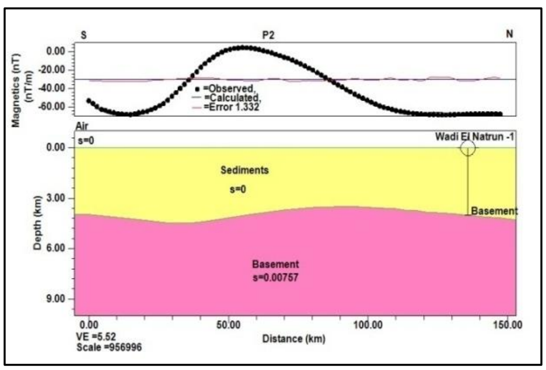

Figure 13. 2D modeled magnetic profile 2 of the investigated area.

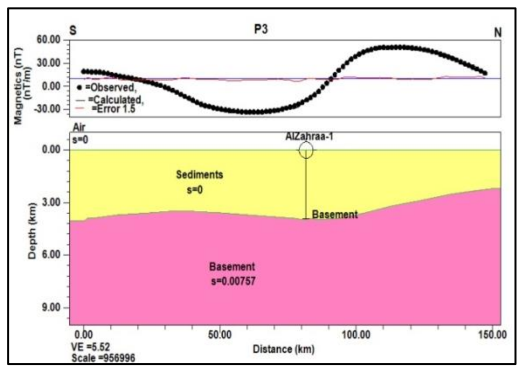

Figure 14. 2D modeled magnetic profile 3 of the investigated area.

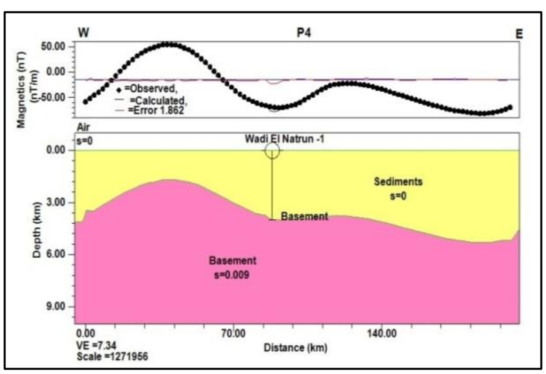

Figure 15. 2D modeled magnetic profile 4 of the investigated area.

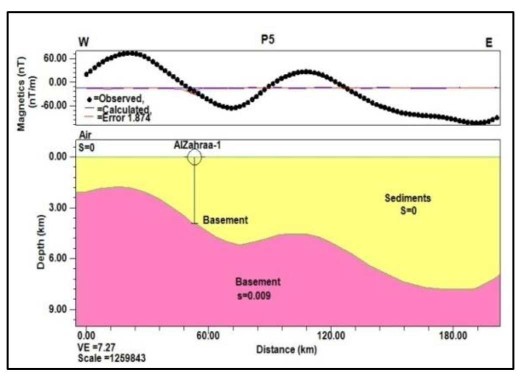

Figure 16. 2D modeled magnetic profile 5 of the investigated area.

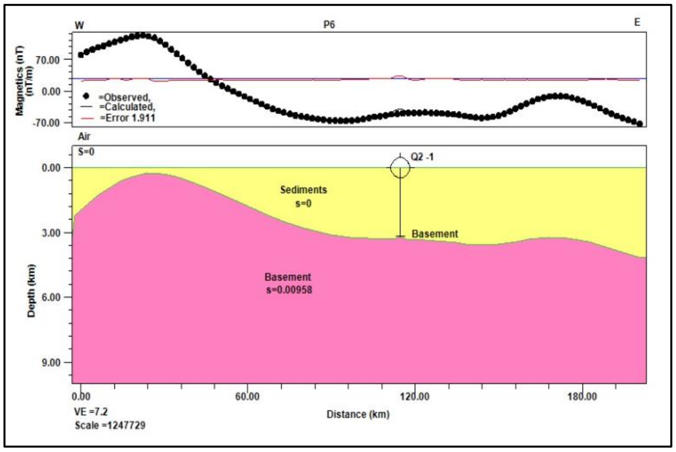

Figure 17. 2D modeled magnetic profile 5 of the investigated area

4. Conclusion

According to the study results, the total Intensity Magnetic Map is decreased to the northern magnetic pole (RTP). The regional-residual separation is used on the reduction to magnetic pole map. The deep-seated and shallow magnetic component frequencies can be seen in the power spectrum curve. Regional and residual sources have estimated mean depths of 4.72 km and 1.1 km, respectively. The depths to the basement surface are computed using an examination of the power spectrum curve for each cell of the research area with dimensions of 25 km × 25 km. The structural style of the area derived from the depth map has trends NE-SW, E-W, N-S, NW-SE, and ENE.

Conflict of interest. The authors declare that there are no conflicts of interest regarding the publication of this paper.

ORCID ID

Abd El Nasser R. Abuzied: https://orcid.org/0000-0001-7643-3054

Abdelhay A. Farrag: https://orcid.org/0000-0003-4798-0408

Ali M. Abd-Allah: https://orcid.org/0000-0001-5597-4943

References

Ammar, A.A., Fouad, K.M. & Meleik, M.L. (1988). Evaluation of the Efficiency of Shortend Low-Pass Filters Computed by Inverse Fourier Transform for Potential Fields of Spherical Bodies and Planar Regionals, vol. 1. Faculty of Earth Sciences, King Abdulaziz University, Jeddah, p. 133-148.

Bhattacharyya, B.K. (1965). Two-dimensional harmonic analysis as a tool for magnetic interpretation. Geophysics, 30, 829-857.

EGPC (1992). Western Desert, oil and gas fields (A comprehensive overview). Egyptian General Petroleum Corporation (EGPC), p431.

Garcia, J.G. & Ness, G.E. (1994). Inversion of the power spectrum from magnetic anomalies. Geophysics 59 (3), 391-401.

Geosoft Oasis Montaj (2008). Data Processing and Analysis Systems for Earth Science Applications (Ver. 7). Geosoft Inc., Toronto, Canada. www.geosoft.com.

GM-SYS, (2013). Gravity and Magnetic Modelling Software Part of the Oasis Montaj Software Suite 7. Geosoft Inc., Toronto, Canada. www.geosoft.com

Griffin, W.R. (1949). Residual gravity in theory and practice. Geophysics, 14, 39.

Maurizio, F., Tatina, Q. & Angelo, S. (1998). Exploration of a lignite bearing in Northern Ireland, using ground magnetic. Geophysics, 62(4), 1143-1150.

Schlumberger (1984) In: Geology of Egypt. Paper presented at the Well Evaluation Conference, Schlumberger, Cairo, p1-64.

Spector, A. & Grant, F.S. (1970). Statistical models for interpreting aeromagnetic data. Geophysics, 35, 293-302.

Mekonnen, T.K. (2004). Interpretation and Geodatabase of Dykes Using Aeromagnetic Data of Zimbabwe and Mozambique, M.Sc.Thesis, p.80.

Mostafa, A.R, Abdel Aziz, M. & Gabber, W. (2008). Tiba- Natrun - Kattaniya Basin, Northern Western Desert (Egypt): Impact of Fault Orientations on Basin Inversion, vol.1. Geology of East Libyia, p.295-310.

Talwani, M., Worzel, J.L. & Landisman, M. (1959). Rapid gravity computations for two dimensional bodies with application to the Mendocino submarine fracture zone. Journal of Geophysical Research, 64, 49-59.

Talwani, M. & Heirtzler, J.R. (1964). Computation of magnetic anomalies caused by two-dimensional bodies of arbitrary shape. In: Parks, G.A. (Ed.), Computers in the Mineral Industries, Part 1, and vol. 9. Stanford University Publications, Geological Sciences, p. 464-480.